Korean Journal of Remote Sensing, Vol.26, No.6, 2010, pp.645~652

CCD Signal Processing for Optimal Non-Uniformity Correction

Jong-pil Kong* and Song Jae Lee †**

*Korea Aerospace Research Institute, 45 Eoeun-Dong, Daejeon, 305-333, Korea

**Dept. of Electronics Engineering, Chungnam National University, Daejeon, 305-764, Korea

Abstract : The performance of the payload Electro-Optical System (EOS) in satellite system is affected by various factors, such as optics design, camera electronics design, and the characteristics of the CCD (Charge Coupled Device) used, etc. Of these factors, the camera electronics design is somewhat unique in that its operational parameters can be adjusted even after the satellite launch. In this paper, the effect of video gain on the non-uniformity correction performance is addressed. And a new optimal non-uniformity correction scheme is proposed and analyzed using the data from real camera electronics unit based on a TDI (Time Delayed Integration) type of CCD. The test results show that the performance of the conventional non-uniformity correction scheme is affected significantly when the video gain is added. On the other hand, in our proposed scheme, the performance is not dependent on the video gain. The insensitivity of the non-uniformity performance on the video-gain is mainly due to the fact that the correction is performed after the dark signal is subtracted from system response.

Key Words : EOS, CCD, NUC, DNSU, PRNU.

1. Introduction

The Electro Optical System (EOS) as a payload in a satellite system consists of Optical Module (OM) and CEU (Camera Electronics Unit) which uses CCD (Charge Coupled Device) as a key component. In general, the performance of the EOS is largely dependent on the design of both OM and CEU. In the case of OM, it is almost impossible, once the satellite is launched, to modify its design. In the case of CEU, however, various operational parameters can be adjusted, even after the launch, to compensate the performance degradation resulting mainly from the aging effect of the electronics (Srour 1988). The correction parameters are often uploaded by ground station using operational command. The most important correction parameters among them are the video gain, offset, and non-uniformity correction parameters required to obtain optimized images. It is noted that the non-uniformity correction should be done in orbit because, when the non-uniformity performance is poor, the subsequent data compression removes dominantly the high spatial frequency components and thereby changes the

Received November 4, 2010; Revised December 20, 2010; Accepted December 24, 2010.

† Corresponding Author: Song Jae Lee (SJLEE@cnu.ac.kr)

characteristics of the original image (Majid and Raul 1991). In this paper, we discuss the in-orbit non-uniformity correction with video gain applied and propose the optimized correction scheme to avoid the adverse effect due to the applied video gain. For the verification we analyzed the real measurement data from the CEU, which was built based on the CCD module from *Fairchild Imaging*. The test result shows that the non-uniformity performance is degraded significantly in the conventional scheme by the video gain but is not affected in the proposed scheme. The improved performance in the proposed scheme is mainly due to the fact that the non-uniformity correction is performed after the dark signal correction, in which the dark signal is subtracted from the measured data so that the system response is more linear and thus the adverse effect of the offset on the non-uniformity correction is minimized.

2. Overview of the CEU

As shown in Fig. 1, the CEU block consists of a 4K CCD and its peripheral electronics. The CCD from *Fairchild Imaging* is TDI (Time Delay Integration) type. The two key components of the peripheral electronics are the CSP (CCD Signal Processor, AD9824) from *Analog Device, Inc*. with input range of 1V and LVDS (Low Voltage Differential Signal) data serializer. Most of the functional units in the CEU including the DSNU and PRNU (Photon Response Non-uniformity) correction, and the interface with EGSE (Electronic Ground Support Equipment) are implemented inside a FPGA. The EGSE, the CEU controller for the ground test, sends the commands for imaging, and receives both the raw image data and telemetry from CEU. The conceptual signal flow from the CCD output to the CEU output is depicted in Fig. 2. The analog output from the CCD is transferred to the CSP, in which the CDS (Correlated Double Sampler) samples the reset noise and signal sequentially and then subtract reset noise from the signal (Albert 1996, Gerld 1998). The VGA (Video Gain Amplifier) in the Fig. 2 often works to balance the output level differences among the output ports due to different CCD amplifiers. At the same time it also works to amplify the signal level as well. It is noted, however,

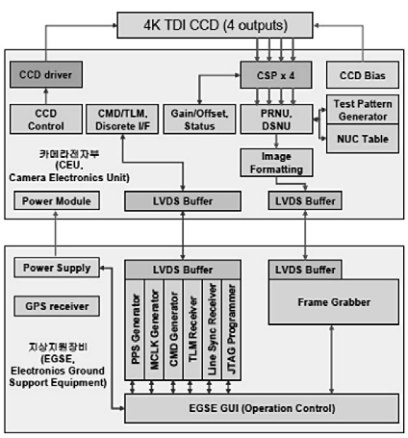

Fig. 1. CEU System Block Diagram.

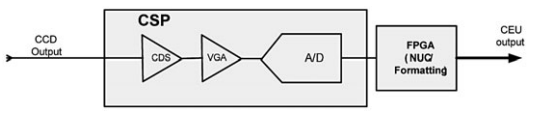

Fig. 2. Flow of CCD Signal Processing.

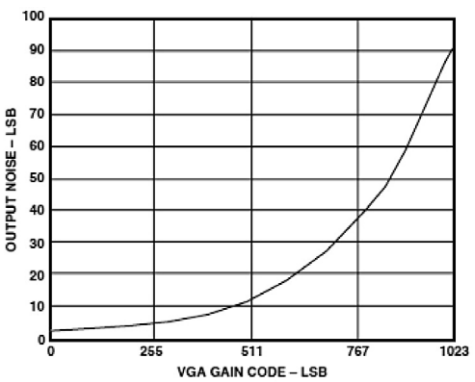

Fig. 3. Output Noise vs. VGA Gain.

that the VGA introduces noises that increase exponentially with the applied video gain as shown in Fig. 3. Thus, it would be, in general, better not to use it unless required in certain reasons. It is noted that on-board corrections such as the dark signal correction, non-uniformity corrections were not performed to obtain the raw image data that has been used in the analysis.

1) CCD architecture

The CCD5045 from *Fairchild Imaging* shown in Fig. 4 was adopted as the key component of CEU (*Fairchild Imaging* 2004). It is a TDI type line scan sensor that has the pixel size of $13\mu m \times 13\mu m$ and 4096 active pixels per line. Four separate output ports are provided to achieve fast operation up to 30.6 KHz. Depending on the exposure level, both the scan rate and TDI levels of 96, 64, 32, 16 or 4 are selectable by commands. The data from both three dummy pixels and active pixels are transferred serially through a horizontal resistor to be collected at each output port. Important CCD parameters, such as the saturation charge, Quantum Efficiency (QE) and readout noise, etc. are summarized in the Table 1. Based on the saturation charge and the sensitivity of output amplifier, the maximum input voltage to the CSP is calculated to be around 0.6 *V*, which is A/D-converted to 9,830 ADU (Analog Digital Unit). However, the maximum input range of the CSP is 1 *V* corresponding to 16,384 ADU without any gain inside CSP.

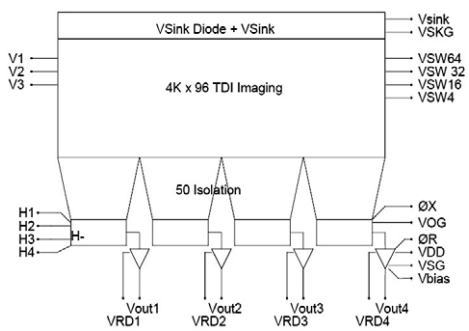

Fig. 4. CCD Block Diagram.

Table 1. CCD Characteristics

Description	Min.	Typical	Max.	Unit
Saturation charge	150	200	-	Ke
QE at 650 nm	20	22	-	%
Readout noise	-	70	100	e
PRNU	-	5	10	%
Dark Current	-	1	-	nA/cm^2
DSNU	-	<5%	-	Qsat
Output AMP Sensitivity	2.5	3	3.5	μV/e-

3. CCD Noise Classification

Many noise models were found in literatures (James 2001, Heli 2005, Gerld 2002). The models are classified into three categories. The one category is associated with the PTC (Photon Transfer Curve) and includes read noise, signal shot noise and fixed pattern noise of PRNU. Read noise represents the random noise measured under totally dark condition and includes on-chip amplifier noise and any other noise sources that are independent of the signal level like dark current shot noise. Reset noise, thermal noise and 1/f nose belong to this noise. Signal shot noise becomes dominant as the signal level reaches the middle range of input and is characterized by a line of slope 1/2 on logarithmic scale because this noise increases in proportion to the square-root of the input signal level. The pattern noise associated with PRNU increases with input signal and becomes prominent under high illumination level. The PTC curve for read noise, shot noise and fixed pattern noise is shown in the Fig. 5. Lastly, PRNU refers to pixel-to-pixel variation in response to uniform input. And thus it is a signal dependent noise and is function of a multiplication factor of the photoelectron number. On the other hand, DSNU refers to the pixel-

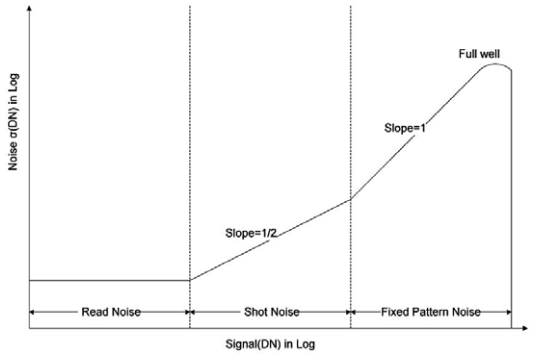

Fig. 5. Photon Transfer Curve.

to-pixel variation in response under dark condition. It is primarily due to dark current differences among pixels. And thus, it is a signal-independent noise and is additive to the other noise power.

4. Non-Uniformity Correction

Many calibration-based non-uniformity correction schemes are introduced (John and Yu-Ming 1999, Yaobo *et al*. 2006, Tao *et al*. 2009). Most of them are based on the ideal photoelectrical response model of CCD. The linear photo electrical response model for ideal pixel is given by

$$y = ax + b \tag{1}$$

where y, x, a, b are the output signal, input illumination, photo responsibility gain and offset, respectively. In reality, no pixels in CCD are ideal and their photoelectrical behaviors would be deviated from the ideal one. In this case, the response for the *i-th* pixel may be expressed by

$$y_i = a_i x + b_i. \tag{2}$$

The deviation of y_i from y indicates the difference of the characteristics between the real and ideal pixels. The compensated response S_i for the *i-th* pixel, which should have the same ideal response y, would be expressed by

$$S_i = P_i y_i + D_i = \frac{a}{a_i} y_i + (b - \frac{a}{a_i} b_i) = y. \tag{3}$$

$$P_i = \frac{a}{a_i} \tag{4}$$

$$D_i = b - \frac{a}{a_i} b_i \tag{5}$$

The adjustment parameters P_i and D_i would be called the non-uniformity gain compensation and offset compensation, respectively. From the equations (3), (4) and (5), we can see that non-uniformity correction is achieved by multiplying raw data by non-uniformity gain parameter and then adding offset parameter. Tao *et al*. (2009) showed that when video gain g_x applied output S_{gxi} is given by

$$\begin{aligned} S_{gxi} &= P_{gxi} g_x y_i + D_{gxi} \\ &= P_{gxi} g_x a_i x + P_{gxi} g_x b_i + D_{gxi} \\ &= g_x (P_{gxi} a_i x + b) = g_x (ax + b) \end{aligned} \tag{6}$$

$$P_{gxi} = \frac{a}{a_i} = P_i \tag{7}$$

$$D_{gxi} = g_x b - P_{gxi} g_x b_i = g_x (b - \frac{a}{a_i} b_i) = g_x D_i \tag{8}$$

where P_{gxi}, D_{gxi} denotes non-uniformity gain and offset parameters for the *i-th* pixel, respectively, when the video gain is applied. We can see, from equations (3) ~ (8), that the non-uniformity offset parameter D_{gxi} is different from D_i whereas the non-uniformity gain parameter P_{gxi} is the same as P_i. The conventional signal flow diagram for data correction, when a video gain is applied, is described in Fig. 6. It is noted, in this scheme, an additional multiplication process is required in the offset parameter calculation using a modification factor that is a function of the

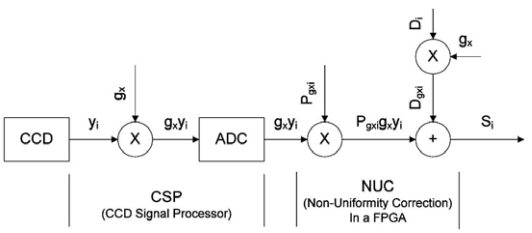

Fig. 6. Conventional Non-uniformity Correction Scheme.

applied video gain in order to accommodate the modification. In Fig. 6, the non-uniformity correction parameters are stored in an electrically programmable memory so as to be updated when it is necessary to compensate for the effect of aging of the camera system after the launch.

5. Proposed Non-Uniformity Scheme

In general, the offset b_i in equation (2) is not a constant, because it changes as a function of temperature and integration time of light energy that is controlled by scan rate, etc. In this case, the equation (2) is rewritten by

$$y_i = a_i x + b_i + \Delta b(t) \tag{9}$$

where b_i is the part of the offset that is assumed to be constant for the *i-th* pixel and $\Delta b(t)$ is the time-dependent part of the offset, which we assume to be the same for all the pixels. Then, the corrected signal, S_{gxi} will be expressed by

$$S_{gxi} = P_{gxi} g_x y_i + D_{gxi} + P_{gxi} g_x \Delta b(t) \tag{10}$$

We know, from equation (10), that the term $P_{gxi} g_x \Delta b(t)$ would remain even after the non-uniformity correction leading to non-uniformity still existing among pixels.

Fig. 7 shows the improved non-uniformity correction scheme proposed in this study. In this scheme, DSNU, non-uniformity under the dark condition, is corrected first after subtracting the dark signal level from each pixel and making the system response more linear, and next PRNU, non-uniformity under light illumination, is corrected. In addition, we used a digital video gain G_x inside CSP, instead of analog video gain that would induce extra noise. Another advantage of employing digital video gain is that the gain can be combined with non-uniformity gain parameter $P_i = a/a_i$ to obtain $G_x P_i = G_x \times a/a_i$. With dark signal correction performed by subtracting the average of output levels of dark pixels at both edges of the CCD lines, the ideal photo-response model of CCD pixel would have no offset and is simply expressed by

$$y = ax \tag{11}$$

where y, x, a denote output signal of CCD, input illumination and photo responsibility gain of ideal pixels respectively. As a consequence, the correction in our proposed scheme begins with removing time-varying offset, $\Delta b_i(t)$. Next, it subtracts DSNU value, b_i of each pixel in a CCD lines, and then compensates for the PRNU by multiplying PRNU parameter a/a_i of each pixel as shown in Fig. 7. In this way, DSNU is treated before applying video gain, and thus only PRNU parameter that is not affected by video gain is associated with application of video gain. As a result, in our proposed scheme, the video gain will not affect the non-uniformity correction.

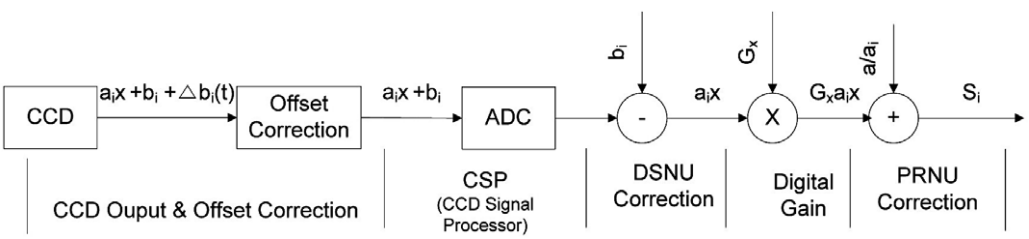

Fig. 7. Proposed Non-uniformity Correction Scheme.

6. Test Results

In this section we present the test results. In addition, we verify that the non-uniformity performance in the proposed non-uniformity correction scheme is not affected by the video gain whereas the conventional scheme is affected. The test has been performed on the image data from the real CEU explained in section 2. We have used three different integration time with TDI level fixed to 16 to acquire different signal level. Two levels have been used for calculating the non-uniformity correction parameters and the rest has been used for the non-uniformity performance evaluation. The effect of the video gain on the non-uniformity correction was compared between the conventional and proposed schemes.

1) Test Set-up and Integration Time

The test set-up for gathering image data is shown in the Fig. 8. Both the integrating sphere and CEU explained operate under the control of EGSE. We varied the integration time to obtain different signal levels. Integration times of 70 μs and 660 μs (or 220 μs) were set to capture the dark image and reference image under illumination, respectively. Then, the both images were used for calculating non-uniformity parameters. Integration time of 220 μs (or 660 μs) was used to capture an image for non-uniformity evaluation. For both the calculation of non-uniformity parameters and the evaluation of non-uniformity, 1,000 lines were captured and averaged to remove the random noise components. And only one out of four output ports was used to eliminate the difference in the output characteristics due to different amplifiers. Fig. 9 shows the dark image signal levels from four different output ports. The upper one shows a two-dimensional dark image with 1000 lines × 4096 pixels and the lower one shows the signal level averaged over 1000 lines for each pixel. It can be noticed, from Fig. 9, that the signal levels from first and second output ports are higher than those from third and fourth output ports. The Table 2 shows the statistics of the image data from each output port under dark illumination, and we can see that the standard deviation is the smallest in the pixels through the second output port.

Fig. 10 shows 2-dimensional image captured under uniform illumination with the integration time of 660 μs. The signal level is around 11,000 ADU. The statistics of the image from each output ports under illumination condition are presented in the Table 3.

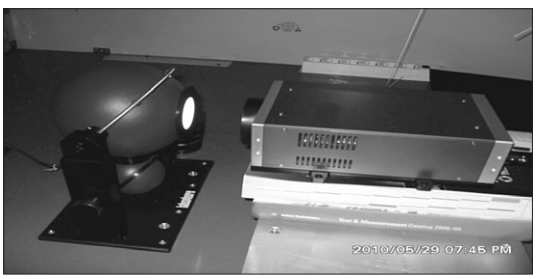

Fig. 8. Test set-up for Capturing Image Data.

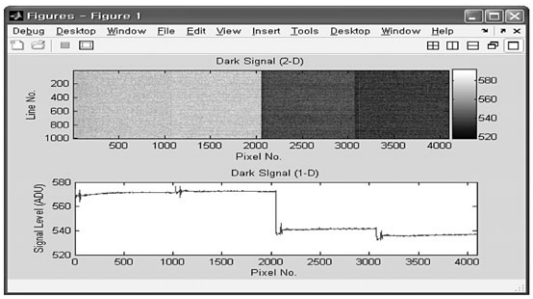

Fig. 9. 2-D Dark Image and Signal Level.

Table 2. Statistics Comparison of Dark Image between Outputs

Parameter	Outport#1	Outport#2	Outport#3	Outport#4
Mean	571	572	541	536
Max.	574	577	546	540
Average	564	567	536	532
S.D	1.011	0.49	0.91	0.76

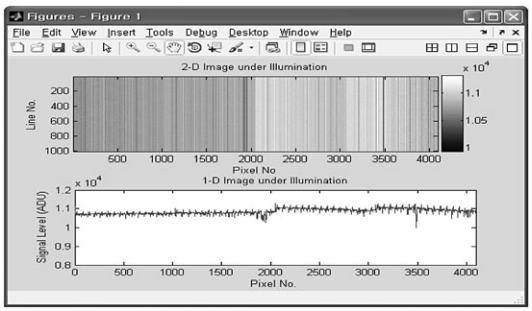

Fig. 10. 2D-Image and Signal Level under Illumination.

Table 3. Statistics Comparison of Illuminated Image between Outputs

Parameter	Outport#1	Outport#2	Outport#3	Outport#4
Mean	10719	10770	10974	10956
Max.	11120	11012	11291	11264
Average	10489	10274	10605	9995
S.D	51.6	81.3	75.7	128.6

2) Non-Uniformity Evaluation

There are different methods for non-uniformity evaluation (ESA/SCC Group 1993). We used the non-uniformity evaluated by

$$Non\text{-}Uniformity\,(\%) = \frac{S.D}{Average} \qquad (12)$$

where we note that the standard deviation (*S.D*) is used in the numerator to minimize the effect caused by some abnormal pixels on the evaluation result. Fig. 11 and Fig. 12 show non-uniformity correction results from the conventional and proposed scheme, respectively. In both figures, the upper left plot shows the signal level of pixels 1025 to 2049 in second output port, before non-uniformity correction without video gain. The upper right plot shows the same image taken after non-uniformity correction. Each

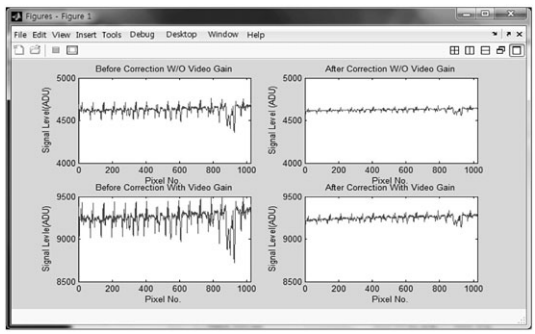

Fig. 11. Non-Uniformity Comparison before/after Correction by Conventional Scheme.

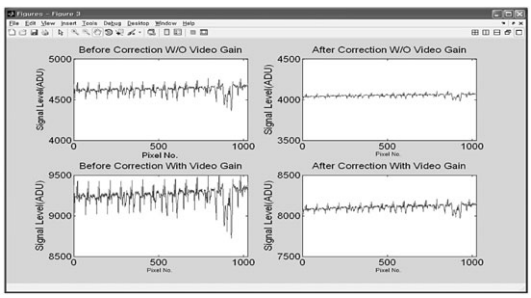

Fig. 12. Non-Uniformity Comparison before/after Correction by Proposed Method.

signal level of each pixel was averaged over 1000 lines to eliminate the random noise. The lower left plot shows the signal level of each pixel before non-uniformity correction and the lower right plot show the one after non-uniformity correction with video gain applied. The non-uniformity test results are summarized in Table 4. It is noted that the both the dark image and the image with integration time of 660 μs for calculation of non-uniformity correction parameter were taken from Test A. Then, the non-uniformity evaluation was performed on the image using integration time of 220 μs. On the other hand,

Table 4. The Summary of Non-Uniformity Comparison between Conventional and Proposed Scheme

Test	Correction Scheme	W/O gain, Before NUC	W/O gain, After NUC	With gain, Before NUC	With gain, After NUC
A	Conventional Scheme	1%	0.33%	1%	0.29%
	Proposed Scheme	1%	0.38%	1%	0.38%
B	Conventional Scheme	0.75%	0.36%	0.75%	0.39%
	Proposed Scheme	0.75%	0.38%	0.75%	0.38%

*NUC (Non-Uniformity Correction)

the dark image and the image with integration of 220 μs were taken for calculation of non-uniformity correction parameter and the image with integration of 660 μs was taken for non-uniformity evaluation for Test B. We can see, from both tests, that the non-uniformity after correction is constant at 0.38 % in the proposed correction scheme, regardless of application of video gain; whereas the non-uniformity in the conventional correction scheme changes from 0.33 % to 0.29 % in the test A and from 0.36 % to 0.39 % in the test B, respectively.

7. Conclusion

A new signal processing scheme for the non-uniformity correction was proposed in this study. The performance of the proposed scheme was compared with the conventional scheme. The improvement over the conventional one was verified by analysis based on the real measurement data obtained using real CEU built with a TDI-type linear CCD. We showed that performance of the non-uniformity correction becomes poor in the conventional scheme as a result of the offset when video gain is applied, whereas the non-uniformity is constant in proposed scheme regardless of the video gain applied. It is noted, however, that the proposed scheme assumed the perfect removal of the dark signal in order to make the system response linear. But this assumption is hardly implemented in real hardware and this aspect should be addressed in practical application.

Reference

Albert, J. P. T., 1996. Solid-State Imaging with Charge-Coupled Device (Kluwer Academic Publisher), P.219.

ESA/SCC group, 1993. Electro-Optical Test Methods for Charge Coupled Device, P23-24.

Fairchild Imaging, 2004.CCD5045 Time Delay Integration Line Scan Sensor data sheet.

Gerald, C. H., 2002. Electro-Optical Imaging System Performance (SPIE), P.320.

Gerald, C. Holst, 1998. CCD Arrays, Cameras, and Displays (SPIE Optical Eng. Press), P.123.

Heli, T. Hytti, 2005. "Characterization of digital image noise properties based on RAW data" SPIE and IS&T.

James, R. Janesick, 2001. Scientific Charge-Coupled Devices, Bellingham (SPIE).

John, G. Harris and Yu-Ming, Chiang, 1999. IEEE Transactions on Image Processing, 8(8).

Majid, R. and Raul, W. J., 1991. Digital Image Compression Techniques (SPIE), P.102.

R. Srour, 1988. Proceeding of the IEEE, P1143-1469.

Tao, Li, Mingyi, He, Ning, Lei, Chunmei, Li, and Qingyuan Wang, 2009. ICIEA2009, p.1483.

Yaobo, J., Shuangcheng, R., Huixin, Z., and Chengxiang, L., 2006. Proceedings of the 6th World Congress on Intelligent Control and Automation.